CHAPTER 9 DISCUSSION

9.1 Effect of molybdenum additions on the continuous cooling transformations

9.1.1 Effect of molybdenum on polygonal ferrite formation

(i) With no prior deformation

From figures 7.22 and 7.24 (in section 7.4 above), it is evident that the polygonal ferrite region in the CCT diagram is more extended at the expense of the pearlite region in alloy #5 (with 0.22% Mo) than in the Mo-free alloy #6 for a condition of no prior deformation. From these figures it may be concluded that the temperature range for polygonal ferrite formation is enlarged in the case of alloy #5 with an 0.22% Mo addition, although the cooling rate range for polygonal ferrite formation is very similar (ranging from 0.1 to 4 $^{o}Cs^{-1}$ for alloy #6 and from 0.1 to 5 $^{o}Cs^{-1}$ for alloy #5). Formation of pearlite takes place within the cooling rate range of 0.1 to 1.5 $^{o}Cs^{-1}$ for the Mo-free alloy #6. Pearlite, however, can be observed between the cooling rates of 0.1 and 0.4 $^{o}Cs^{-1}$ with an 0.22% Mo addition in alloy #5. This is clearly due to the Mo addition in the alloy. Molybdenum is a ferrite forming element and diminishes the austenite phase field[97]. It can, therefore, promote polygonal ferrite and hinder pearlite formation under no prior deformation conditions in austenite.

(ii) With prior 45% reduction deformation at 860 ^{o}C below the T_{nr}

A similar result was obtained with a prior 45% reduction deformation in alloys #5 and #6 (see figures 7.28 and 7.26 in section 7.5). Polygonal ferrite was observed after all cooling rates, but formed within a wider temperature range in alloy #5 (with 0.22% Mo) than in the Mo-free alloy #6 during continuous cooling. The transformation temperature range for pearlite formation, however, was suppressed in alloy #5 (with 0.22% Mo) in the case of a prior deformation (see figure 7.28). This was an indication that the pearlite formation region was reduced by the molybdenum addition. It can, therefore, be concluded that molybdenum addition to Nb-containing low carbon line pipe alloys with prior deformation, promotes the formation of polygonal ferrite and inhibits pearlite formation.

9.1.2 Effect of molybdenum on acicular ferrite formation

(i) With a prior deformation

Figure 7.26 shows the strain affected CCT diagram for the Mo-free alloy #6 after solution treatment at 1225 ºC to completely dissolve the Nb(C,N) prior to a deformation of 45% reduction at 860 ºC. The non-recrystallisation temperature T_{nr} of alloy #6 ranged from 900 to 930 ºC and was dependent on the deformation parameters of pass strain, strain rate and inter pass time etc. The deformation prior to cooling for the CCT determination was, therefore, applied in the non-recrystallisation region. Figure 7.26 (in section 7.5) showed that the lowest cooling rate limit for acicular ferrite formation for alloy #6 (Mo-free) was approximately 0.7 $^{o}Cs^{-1}$ while almost the same limit for alloy #5 (0.22% Mo) (figure 7.28 in section 7.5), with a prior 45% reduction, was about 0.5 $^{o}Cs^{-1}$. These two limits for the lowest cooling rates for acicular ferrite formation after prior deformation are, therefore, very close to each other. Furthermore, there was also no measurable difference in cooling rate range (almost 1 to 40 $^{o}Cs^{-1}$) for acicular ferrite formation during cooling between the alloys #5 and #6 (see figures 7.28 and 7.26). It appears, therefore, that a molybdenum addition of about 0.22% Mo to Nb-bearing line pipe alloys does neither promote or retard acicular ferrite formation after a 45% prior reduction at 860 ºC below the non-recrystallisation temperature.

(ii) With no prior deformation

In contrast with the above effects of a prior deformation, the formation of acicular ferrite is affected by molybdenum additions with no prior deformation. The difference can be recognised from figures 7.22 and 7.24 (see section 7.4). Acicular ferrite was found in a wider cooling rate range from 0.1 to 15 $^{o}Cs^{-1}$ for alloy #5 (with 0.22% Mo) if compared to the Mo-free alloy #6 in which the region for acicular ferrite formation was smaller and was observed only within the narrower cooling rate range from 0.3 to 5 $^{o}Cs^{-1}$.

(iii) Conclusions

On one hand there is, therefore, clear evidence that molybdenum additions to Nb-bearing line pipe steels promote acicular ferrite formation under no prior deformation conditions, as has been observed by a number of other researchers[78, 131,163-165]. On the

other hand, the contribution of molybdenum additions appears to be over-shadowed by the effect of deformation in the 0.22% Mo alloy #5 since there was no difference in the AF-forming regions in the CCT diagrams from that of the Mo-free reference alloy #6 (figures 7.26 and 7.28) after a prior deformation below the T_{nr}. It is evident, therefore, that both molybdenum additions and retained strain in the austenite can independently promote acicular ferrite formation. A high density of dislocations induced by the deformation in the austenite prior to transformation is, therefore, beneficial to the nucleation of acicular ferrite. This effect of retained strain on promoting acicular ferrite appears to be stronger than the effect of molybdenum additions.

9.2 Effect of deformation in austenite on acicular ferrite formation

Comparing figures 7.22 (section 7.4) and 7.26 (see section 7.5), the cooling rate range in which acicular ferrite formed, shifted from 0.3 to 5 $^{o}Cs^{-1}$ with no prior deformation, to 0.7 to 40 $^{o}Cs^{-1}$ with prior deformation, for the Mo-free alloy #6. It is, therefore, clear that the acicular ferrite region is expanded due to retained strain in the austenite prior to the phase transformation. It seems that the high density of dislocations in the deformed austenite is beneficial to the formation of acicular ferrite instead of bainite[75]. Bainite formation is completely suppressed in deformed austenite (figures 7.25 and 7.26 in section 7.5). Both bainite and acicular ferrite belong to the group that transform by a displacive transformation[74,76] that may be suppressed by pre-deformation in the austenite[166-168]. From these observations, however, it appears that the bainite displacive transformation must have been suppressed in the deformed austenite whereas the acicular ferrite formation was enhanced.

The main differences between bainite and acicular ferrite formation are related to their nucleation sites and growth directions. Bainite nucleates on austenite grain boundaries and grows as a sheaf of parallel plates with the same growth direction within the austenite grains (figure 7.21-(q) in section 7.4). Acicular ferrite generally nucleates intragranularly on non-metallic inclusions[70, 144,159, 169,170] and grows as primary plates in the same[75,78] or many different orientations[75,76] from these inclusions. Then a new generation of secondary plates nucleates at the austenite/primary acicular plate's interface[75,77]. Consequently, acicular ferrite is characterised by a chaotic arrangement

of plates showing fine grained interwoven morphologies (figure 7.25-(k) to (t) in section 7.5). The grain structures of acicular ferrite laths are also smaller than those of bainite. This may be related to the effect of dislocations adjacent to inclusions/primary plates in deformed austenite that can act as the nucleation sites for secondary plates of acicular ferrite. The retained strain energy[74] in the areas with a high density of dislocations can contribute to the mechanical driving force[51] for acicular ferrite nucleus formation[134]. Dislocations, however, can also hinder the growth of a nucleus of acicular ferrite[76] owing to the displacive nature of the transformation. Thus both of the effects of dislocations of, firstly, promoting nucleation of an acicular ferrite lath and, secondly, suppressing its growth, will lead to an eventual finer acicular ferrite lath structures. Shipway and Bhadeshia[171] have found that a large enough dislocation density in austenite introduced by prior deformation, appears to act as a further nucleation source for Widmanstätten ferrite which forms also by a displacive transformation mechanism, leading to a refinement of microstructure. Sugden[74] has also found that acicular ferrite never grows across austenite grain boundaries.

Figure 7.22 in section 7.4 shows that the cooling rate for the formation of bainite is higher than that required for acicular ferrite. It means that bainite formation requires a higher degree of under-cooling for nucleation, but once it has nucleated, it grows relatively quickly. On the contrary, the undercooling required for the formation of acicular ferrite is lower than that for bainite and its formation might be rate controlled by both nucleation and growth for the primary plates or secondary nucleation on the interface between the plate and austenite. Its transformation model is a mixture of diffusion and shear transformation[4,9,11,43]. Figure 7.22 also shows that the acicular ferrite formation temperature is higher than that of bainite, which is in agreement with the work of Zhao[4] and Kim[11]. This higher transformation temperature is helpful for the carbon diffusion in its rejection from the acicular ferrite primary laths with its lower solubility for carbon than the untransformed austenite.

The same result was obtained in alloy #5 (with 0.22% Mo) (see figures 7.24 in section 7.4 and 7.28 in section 7.5). The bainite transformation was completely suppressed in deformed austenite, while the acicular ferrite formation was promoted, even more with prior deformation than in alloy #6 (Mo-free).

In summary, retained strain in the austenite promotes the nucleation of acicular ferrite, hinders its growth, and at the same time, suppresses the formation of bainite. This results in a shorter lath size of acicular ferrite, which may be beneficial to the toughness of the steel. An addition of 0.22% Mo to Nb-bearing low carbon line pipe steels, therefore, does not markedly affect the formation of acicular ferrite to the same extent as prior deformation of the austenite does.

9.3 Ratio of yield strength to ultimate tensile strength and its effect

The ratio of yield strength to ultimate tensile strength (YS/UTS) is one of the properties sometimes specified for low carbon structural steel. In particular, a low YS/UTS ratio is a very important parameter in the API specifications for line pipe steels as a high work hardening rate is required in this application. In the present work a number of differently alloyed steels treated at various cooling rates, two coiling temperatures and with and without prior deformation in the austenite, were tensile tested in order to establish the relationships between their YS/UTS ratios and these materials and process parameters.

9.3.1 The effect of cooling rate

The cooling rate after austenitisation affects the transformed microstructures that result in different mechanical properties in line pipe steels, such as yield strength (YS), ultimate tensile strength (UTS), elongation and impact toughness. The two alloys #3 (0.09% Mo) and the reference Mo-free alloy #6 were selected for studying the effect of cooling rate on the YS/UTS ratio. The temperature range of varying cooling rates was from 980 ºC down to room temperature.

The effects of cooling rate on the yield strength and ultimate tensile strength are shown in figures 9.1 and 9.2, respectively. Both the yield strength and ultimate tensile strength increase with increasing cooling rate after soaking at 980 ºC, as predicted by the two fitted equations (9.1) and (9.2). The microstructures also changed with cooling rate. Polygonal ferrite dominated the microstructure at lower cooling rates, whereas acicular ferrite plus bainite dominated at high cooling rates. The amount of bainite and acicular ferrite constituents increased with an increase in cooling rate (see figure 7.22 in section 7.4.1) and this increased the strength of the alloy.

$$YS = 4.1CR + 445 \quad \text{(in MPa)} \qquad R^2 = 0.98 \qquad (9.1)$$

$$UTS = 3.9CR + 572 \quad \text{(in MPa)} \qquad R^2 = 0.99 \qquad (9.2)$$

where CR is cooling rate in $^{o}Cs^{-1}$

R^2 is the Regression Coefficient

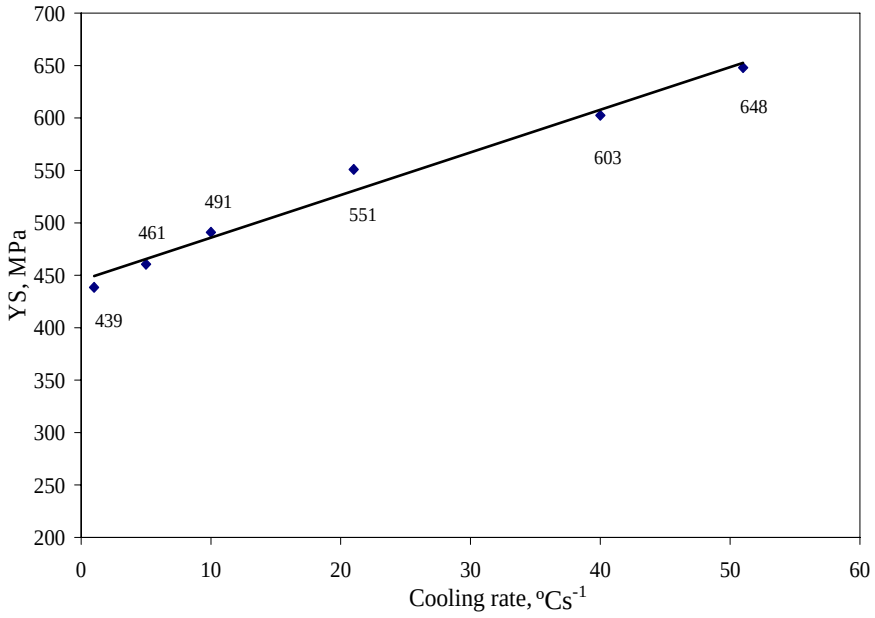

Figure 9.1 The yield strength of the reference Mo-free alloy #6 as a function of the cooling rate from 980 ºC with no prior deformation before the transformation and with no coiling simulation.

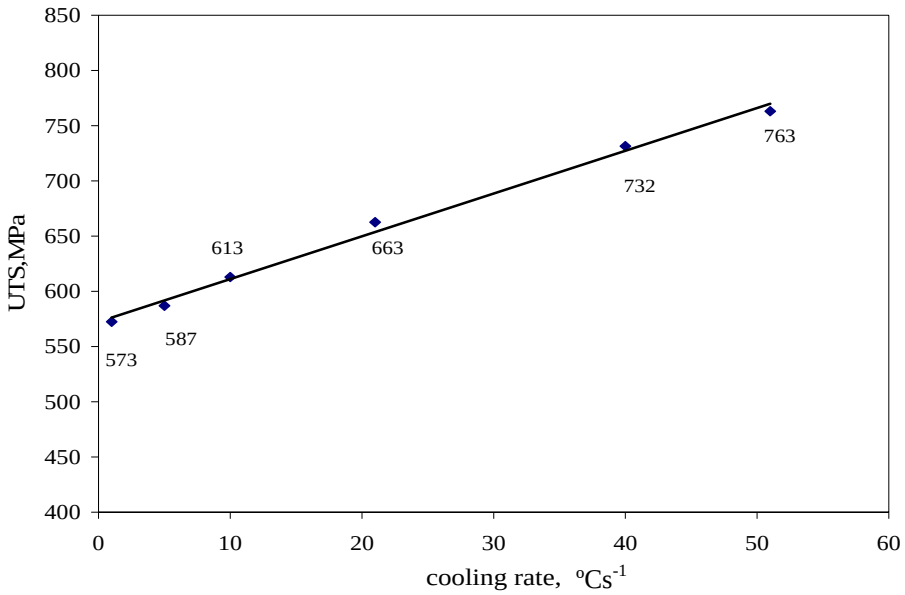

Figure 9.2 The ultimate tensile strength of the reference alloy #6 as a function of cooling rate from 980 ºC with no prior deformation before the transformation and with no coiling simulation.

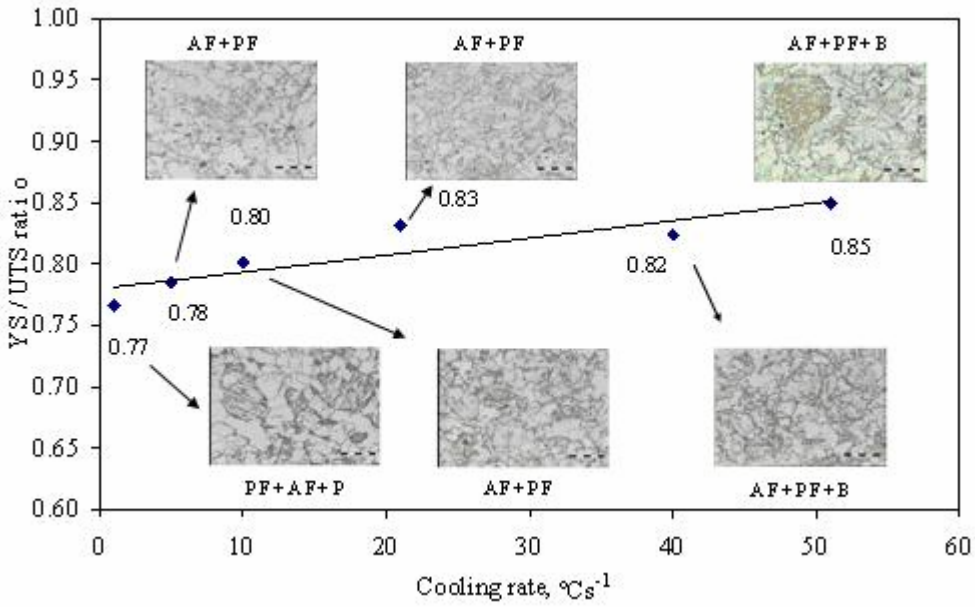

Figure 9.3 The YS/UTS ratio of the reference alloy #6 as a function of cooling rate from 980 ºC with no prior deformation before the transformation and with no coiling simulation. PF-polygonal ferrite, AF-acicular ferrite and P-pearlite.

As may be seen in figure 9.3, it appears that the ratio of YS/UTS increases slowly with increasing cooling rate under conditions of no coiling simulation and no deformation prior to the transformation. Equations (9.1) and (9.2) show that the slope of the YS versus CR line is higher than that of the UTS versus CR, i.e. the cooling rate may affect the YS more than the UTS. This suggests that the dominant structure of acicular ferrite plus bainite could improve the yield strength more than the ultimate tensile strength of these steels. Furthermore, the grain size of the steel will also be finer with increasing cooling rate because of the higher under-cooling at a faster cooling rate. A high density of dislocations and other crystal defects could also have been introduced by an acicular ferrite microstructure or bainite formation due to their displacive formation mechanisms. Such a high density of dislocations has been found in sample #AF3F from alloy #3 with a cooling rate of 40 $^{o}Cs^{-1}$ (seen figure 8.18-(b)). These “prior” defects may interact with other dislocations during early plastic straining, leading to a high yield strength. Therefore, the finer grain size and a high density of dislocations after a rapid cooling rate are useful to raise the YS, thereby increasing the YS/UTS ratio with increasing cooling rate.

A similar result (see figures 9.4 to 9.6) between YS, UTS, YS/UTS and the cooling rate was obtained for alloy #3 containing 0.09% Mo after the same treatment as above for alloy #6. The YS/UTS ratio in alloy #3, however, was not affected to the same degree by the cooling rate as was the case in alloy #6, compare figures 9.6 with 9.3.

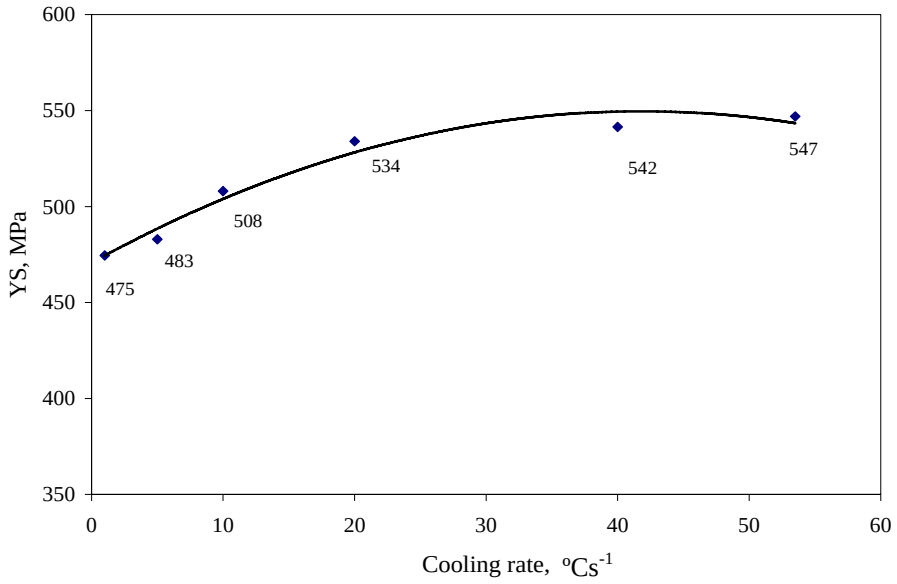

Figure 9.4 The yield strength of alloy #3 as a function of cooling rate from 980 ºC under conditions of no prior deformation to the transformation and no coiling simulation.

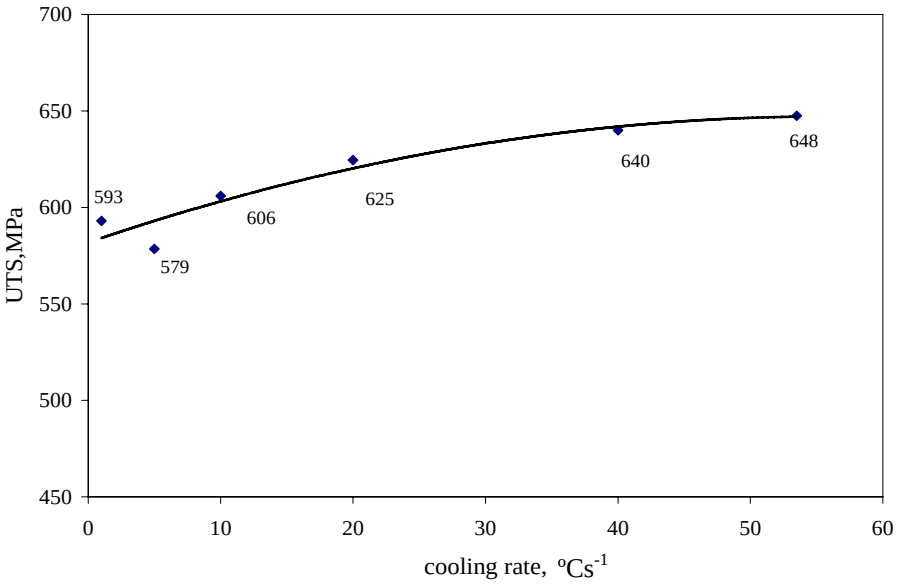

Figure 9.5 The ultimate tensile strength of alloy #3 as a function of cooling rate from 980 ºC under conditions of no prior deformation to the transformation and no coiling simulation.

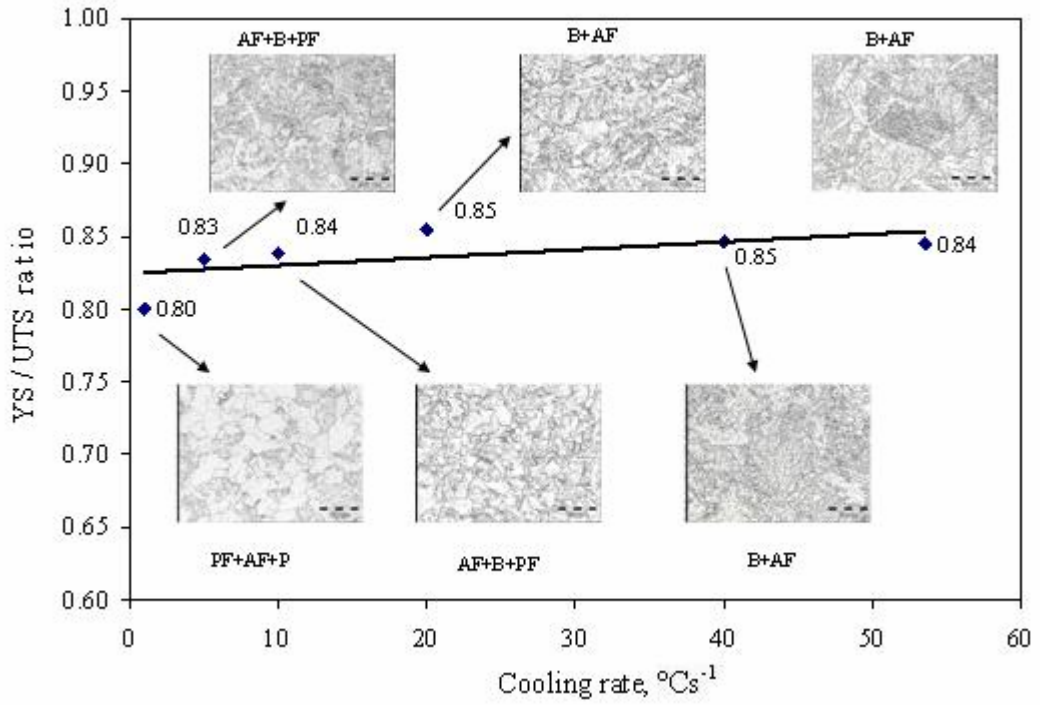

Figure 9.6 The YS/UTS of alloy #3 as a function of cooling rate from 980 ºC under conditions of no prior deformation to the transformation and no coiling simulation. PF-polygonal ferrite, AF-acicular ferrite, B-bainite and P-pearlite

9.3.2 The effect of coiling temperature

Two sets of specimens were treated for coiling simulations at 575 and 600 ºC, respectively, without deformation prior to the transformation. The latter coiling temperature of 600 ºC has recently been lowered to 575 ºC by Mittal Steel SA in their line pipe process. The results of alloy #6 are given in figures 9.7 to 9.9 for the coiling temperature of 600 ºC. It seems that the cooling rate does not markedly affect the yield strength and ultimate tensile strength of this alloy after coiling at 600 ºC. It was observed that the ratio of YS/UTS was also not a function of the cooling rate, with the ratio almost constant, ranging from 0.76 to 0.78. This could be due to the annealing out of the dislocations and other crystal defects introduced by the displacive transformation in acicular ferrite or bainite during the coiling simulation process.

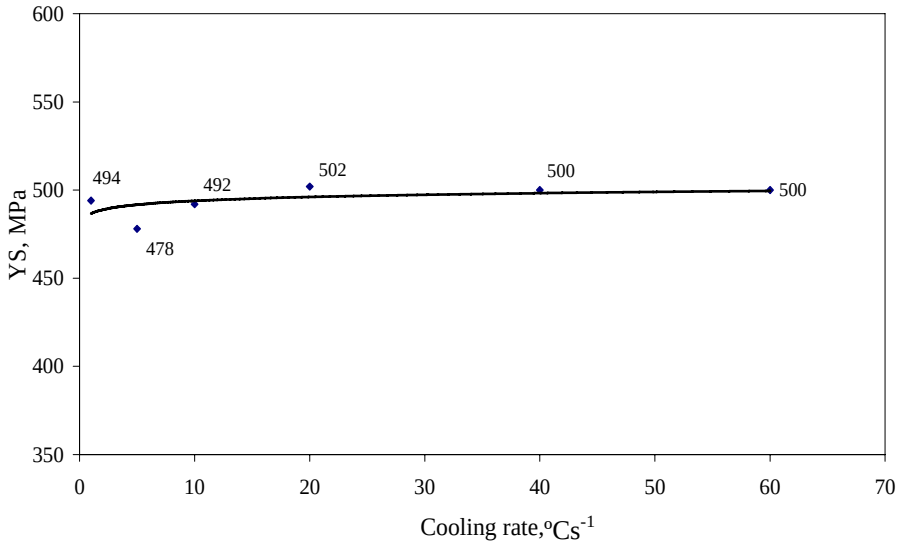

Figure 9.7 The yield strength of alloy #6 as a function of the cooling rate from 980 ºC to 600 ºC under conditions of no prior deformation to the transformation but with a coiling simulation at 600 ºC for 1 hour.

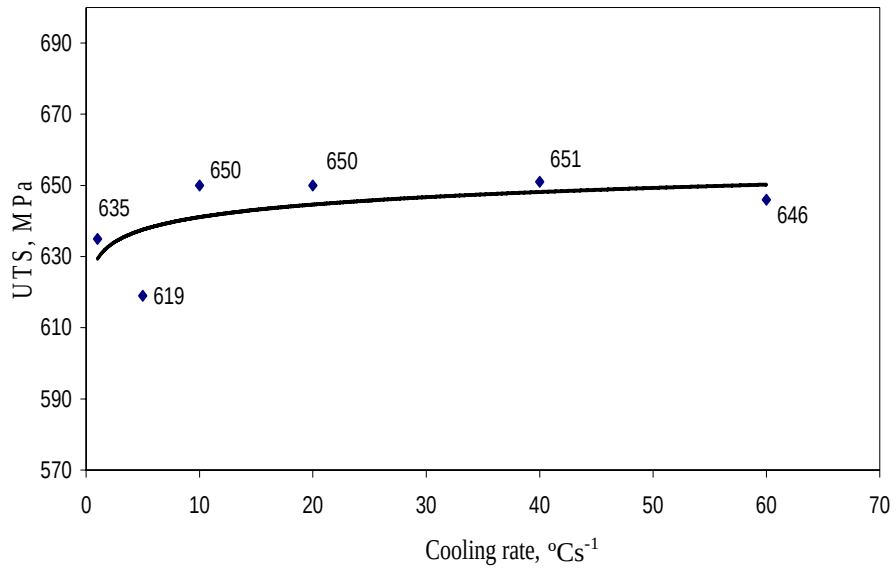

Figure 9.8 The ultimate tensile strength of alloy #6 as a function of cooling rate from 980 ºC to 600 ºC under conditions of no prior deformation to the transformation but with a coiling simulation at 600 ºC for 1 hour.

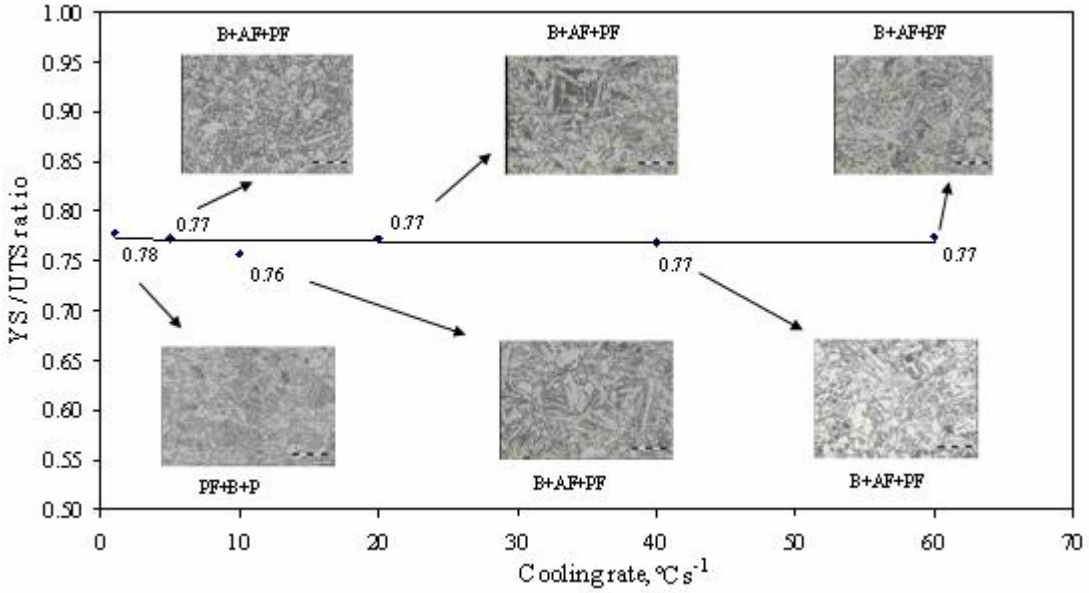

Figure 9.9 The YS/UTS ratio of alloy #6 as a function of the cooling from 980 ºC to 600 ºC under conditions of no prior deformation to the transformation but with a coiling simulation at 600ºC for 1 hour. PF-polygonal ferrite, AF-acicular ferrite, B-bainite and P-pearlite.

Figures 9.10 to 9.12 show the results of the tensile tests of alloy #6 for a coiling temperature of 575 ºC. Similar results were obtained for the coiling simulation at 600 ºC with the ratio of YS/UTS ranging from 0.75 to 0.80. It was concluded that varying the coiling temperature within the range of 575 to 600 ºC did not substantially influence the ratio of YS/UTS for the entire cooling range of 1 to 60 ºCs^{-1}.

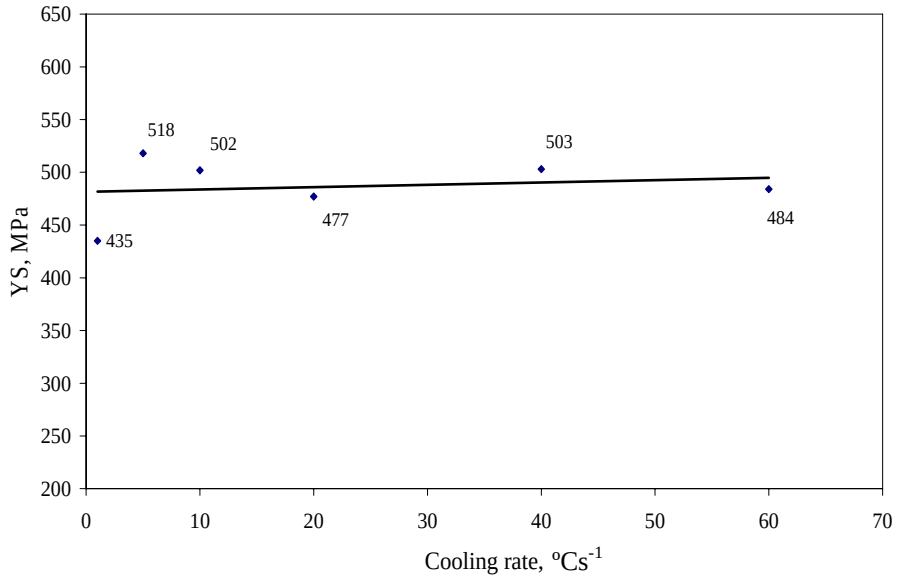

Figure 9.10 The yield strength of alloy #6 as a function of the cooling rate from 980 ºC to 575 ºC under conditions of no prior deformation to the transformation but with a coiling simulation at 575 ºC for 1 hour.

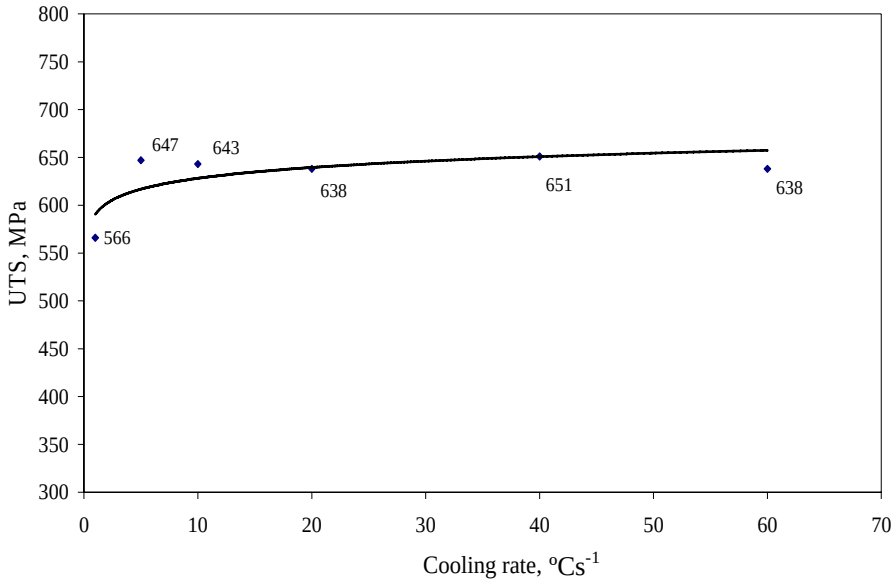

Figure 9.11 The ultimate tensile strength of alloy #6 as a function of the cooling rate from 980 ºC to 575 ºC under conditions of no prior deformation to the transformation but with a coiling simulation at 575 ºC for 1 hour.

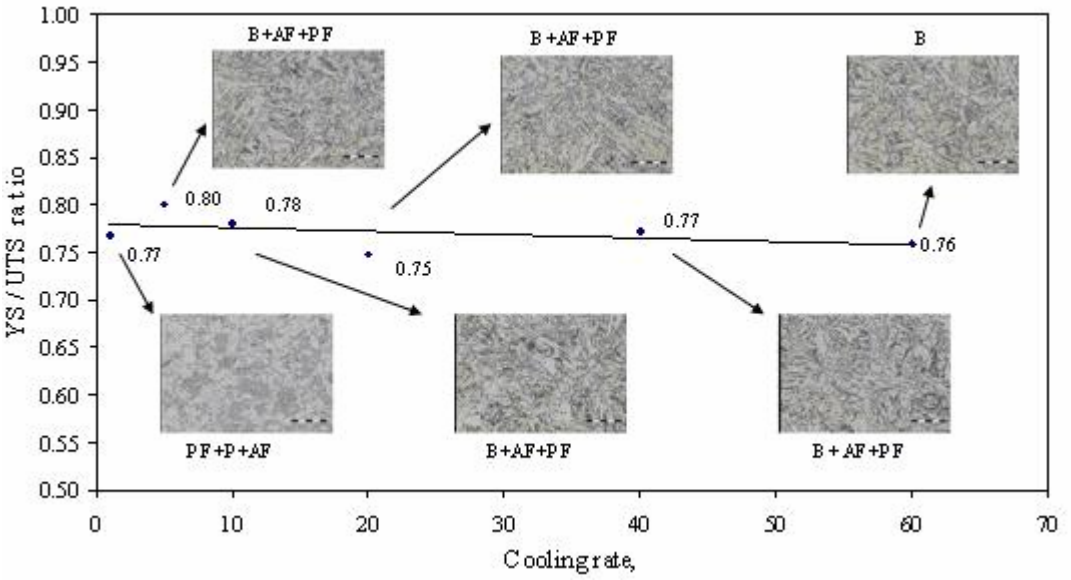

Figure 9.12 The YS/UTS ratio alloy #6 as a function of the cooling rate from 980 ºC to 575 ºC under conditions of no prior deformation to the transformation but with a coiling simulation at 575 ºC for 1 hour. PF-polygonal ferrite, AF-acicular ferrite, B-bainite and P-pearlite.

9.3.3 The effect of prior deformation in the austenite and coiling simulation

This group of specimens was subjected to a deformation in the austenite region with 33% reduction below the T_{nr}, before cooling through the transformation to ferrite from 860 to 575 ºC and then applying a coiling simulation at 575 ºC for 1 hour. The results from these tests are given figures 9.13 to 9.15. As may be seen, the yield strength and ultimate tensile strength were affected by cooling rate as well.

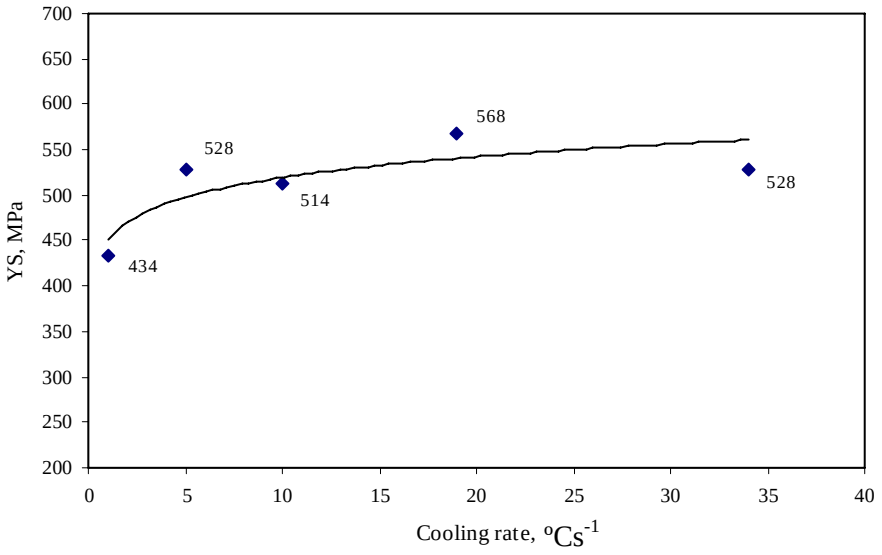

Figure 9.13 Effect of the cooling rate on the yield strength of the reference alloy #6 after prior deformation of 33 % reduction in the austenite below the T_{nr}, cooling to 575 ºC at different cooling rates and simulation of the coiling at 575 ºC for 1 hour.

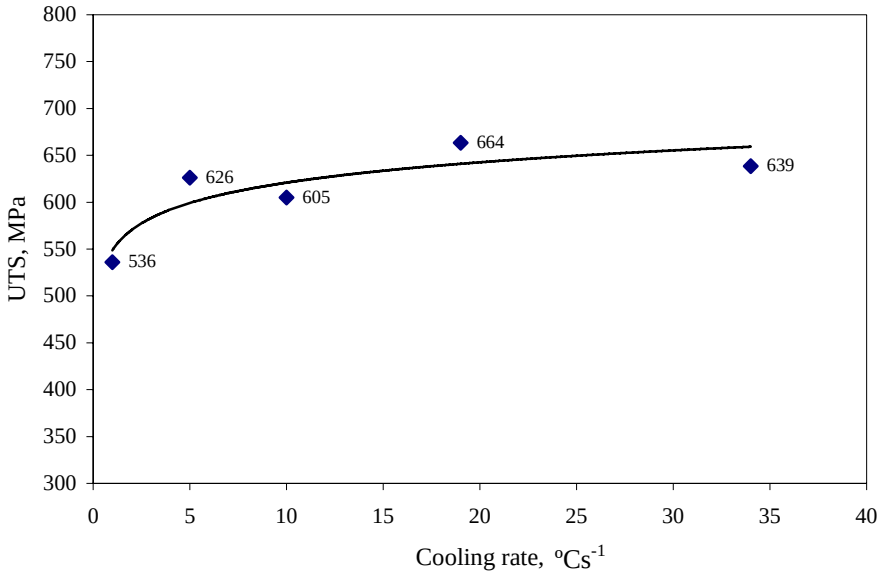

Figure 9.14 Effect of the cooling rate on the ultimate tensile strength of the reference alloy #6 after prior deformation of 33 % reduction in the austenite below the T_{nr}, cooling to 575 ºC at different cooling rates and simulation the coiling at 575 ºC for 1 hour.

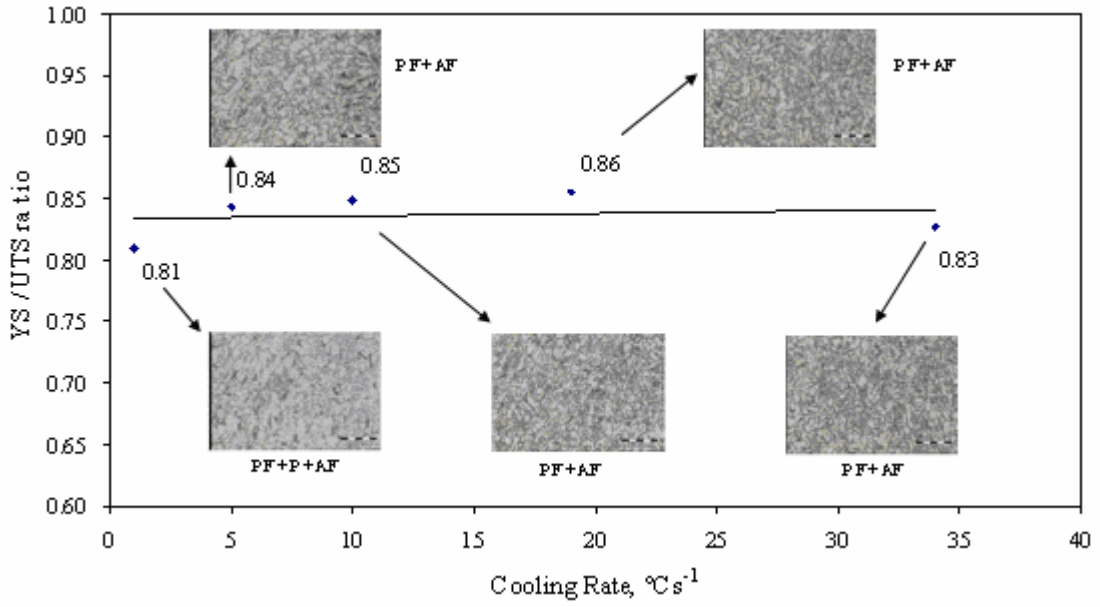

Figure 9.15 Effect of the cooling rate on the YS/UTS ratio of the reference alloy #6 after prior deformation of 33 % reduction in the austenite below the T_{nr}, cooling to 575 ºC at different cooling rates and simulation the coiling at 575 ºC for 1 hour. PF-polygonal ferrite, AF-acicular ferrite and P-pearlite.

Comparing the two cases, in the first case without prior deformation (figure 9.12), a high cooling rate introduces more dislocations into the microstructures because of the acicular ferrite or bainite microstructures which undergo displacive transformation from the austenite. The effect of any difference in dislocation density between a low and a high cooling rate, however, decreased thereafter due to the 60 minutes coiling simulation at 575 ºC, in spite of the fact that a higher dislocation density had initially been introduced by the high cooling rate. In other words, the coiling process decreases the effects of any initial difference in dislocation density in the microstructures caused by low and high cooling rates.

In the case of the prior deformed alloy (figure 9.15), the dislocations are not only from the high cooling rate, but also from the prior deformation. However, the dislocations introduced from the deformation in the austenite do not lead directly to a higher dislocation content in the acicular ferrite, but it does induce a finer (one pass deformation at 1050 ºC above the T_{nr}) and flattened (two passes deformation at 900 and 860 ºC, respectively, below the T_{nr}) austenite grain size that will provide a high nucleation rate of the acicular ferrite during the transformation, leading to a finer

ferrite grain size. The yield strength is sensitive to ferrite grain size[28,172] through the Hall-Petch relationship[174], whereas the ultimate tensile strength is not as sensitive to the grain size[28]. All of these can increase the obstacles for the commencement of plastic deformation and will result in a high yield strength of the steel. Therefore, the YS/UTS ratio could be raised by deformation as it is sensitive to deformation.

Thus, it can be concluded that:

- The YS/UTS ratio was found to be only sensitive to cooling rate or the transformed microstructures in the case without any prior deformation and simulated coiling at 575 and 600 ºC;
- Varying the coiling temperature at 575 and 600 ºC did not affect the YS/UTS ratio but coiling in general diminishes the effect of cooling rate on this ratio;
- Coiling decreases the YS/UTS ratio in the case without prior deformation; and
- A prior deformation of 33% below the T_{nr} in the austenite strongly increases the YS/UTS ratio at all cooling rates from 1 to 34 $^{o}Cs^{-1}$ and overshadows the effect of microstructure or cooling rate.

9.3.4 The effect of acicular ferrite on the ratio of yield strength to ultimate tensile strength

The relationship between the volume fraction of acicular ferrite and the YS/UTS (longitudinal specimens) is shown in figure 9.16. The volume fraction of acicular ferrite was measured on the experimental alloys #1 to #5 after laboratory hot rolling with an 86% reduction and cooling at a rate of 47 $^{o}Cs^{-1}$. These microstructures revealed mainly acicular ferrite mixed with some polygonal ferrite. It appears that the YS/UTS ratio was not markedly influenced by the quantity of acicular ferrite, although the range over which the AF content could be varied, was very limited. This observation is not in agreement with results of other researchers[173] that reported that there is a high density of mobile dislocations in acicular ferrite which result in a high work hardening rate and this lowers the number of obstacles for the commencement of plastic deformation. For instance, Kim has found[172] that increasing the volume fraction of acicular ferrite or bainite is useful to lower the YS/UTS ratio. Tither[173] has also reported that dominating acicular ferrite in a microstructure of line pipe steel could result in a large work hardening rate.

Summarising the above results, it is concluded that varying the acicular ferrite content from both undeformed and deformed austenite in these alloys was not measurably beneficial to lower the YS/UTS ratio, at least not in the quantities used here. An unresolved question remains, however, whether the effect of the quantity of acicular ferrite amount is weaker than that of a prior deformation in austenite? This needs further study with larger variations in the quantity of acicular ferrite than was found possible here.

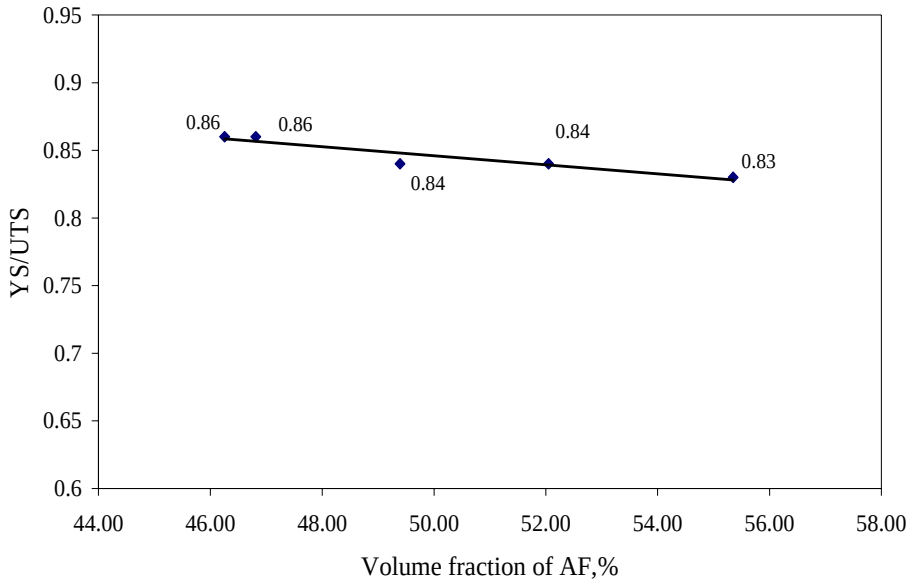

Figure 9.16 Relationship between the YS/UTS ratio (longitudinal specimens) and the measured volume fraction of acicular ferrite in the experimental alloys #1 to #5 after laboratory hot rolling with an 86% reduction in total and rapid cooling at a rate of 47 $^{o}Cs^{-1}$.

CHAPTER 10 CONCLUSIONS

The objective of this study was to establish the relationship between micro-alloying elements, the microstructure and process variables such as cooling rate, prior deformation in the austenite and coiling conditions, on the ratio of YS/UTS and other mechanical properties. Therefore, a study was undertaken on the austenite to acicular ferrite transformation with particular emphasis on the kinetics of the acicular ferrite formation and as affected by the above process variables. The following conclusions could be drawn from the present study:

9.1: The type of undissolved particles are mainly (Ti,Nb)(C,N) and Ti(C,N) after reheating at 1225 ºC for 120 minutes and the smallest size of 46 nm was found in the Nb-Ti-containing reference alloy #6. The volume fraction of undissolved particles decreased with increasing reheating temperatures as follows:

$f_v = 10^{-6} T^2 - 0.0038T + 3.2258$ $R^2=0.97$ for 15 minutes soaking time

$f_v = 10^{-6} T^2 - 0.0043T + 3.3251$ $R^2=0.99$ for 60 minutes soaking time

$f_v = 4\times10^{-6} T^2 - 0.0103T + 6.862$ $R^2=0.97$ for 120 minutes soaking time

9.2: The austenite grain size increased with increasing austenitisation temperature and soaking time. For alloy #6, however, the effect of the temperature is larger than the effect of soaking time. When the temperature reaches above 1225 ºC, coarsening of the particles sets in.

9.3: The non-recrystallisation temperature (T_{nr}) for the Mo-free reference alloy #6 was affected by the pass strain and the inter-pass time. These relationships between the T_{nr} and the pass strain ε and the inter-pass time t_{ip} can be described by the following respective equations:

$$T_{nr} = -210\,\varepsilon + 972$$

$$T_{nr} = 961 t_{ip}^{-0.0128}$$

9.4: The strain-free and strain affected CCT diagrams for alloy #5 (with 0.22% Mo) and alloy #6 (Mo-free), have shown that molybdenum additions can shift the acicular ferrite region on the strain-free CCT diagram to longer times and expand the region

for the formation of acicular ferrite. The dominant microstructures with no deformation in the austenite, were found to have changed from polygonal to an acicular ferrite microstructure and bainite with increasing cooling rate. A 45% deformation in the austenite below the T_{nr} is beneficial to acicular ferrite formation as the deformation promoted the nucleation of an acicular ferrite microstructure and hindered the growth of its constituents at the same time, and substantially suppressed the transformation to bainite. The effect of molybdenum additions on acicular ferrite transformation in these steels is overshadowed by the stronger effect of the prior deformation in alloys #5 (with 0.22% Mo) and the Mo-free reference alloy #6.

9.5: The transformed microstructures of all alloys were found to be a mixture of polygonal ferrite plus an acicular ferrite microstructure. The technique of TEM examination of shadowed carbon extraction replicas was found to be a superior method to identify these microstructures, rather than optical microscopy and SEM.

9.6: The acicular ferrite microstructure in the present study was found to have a lath morphology with two types: parallel laths and interwoven laths but with the more typical one of parallel laths. A high density of dislocations was found inside the laths. However, no cementite was observed between laths and within the laths. The nucleation sites for acicular ferrite were often oxide and sulphide inclusions with mostly round shape and the observed sizes of these inclusions ranged from 0.35 to 2.2 μm.

9.7: The YS/UTS ratio ranged from 0.83 to 0.86 for the alloys with microstructures of polygonal ferrite plus acicular ferrite after hot rolling and rapid cooling. However, an acicular ferrite microstructure or bainite was found to be not beneficial in lowering the YS/UTS ratio. This ratio was only sensitive to the microstructure or the cooling rate in the case with no prior deformation and without any simulated coiling process. The YS/UTS, yield strength and ultimate tensile strength by themselves, however, were not sensitive to the cooling rate after a simulated coiling process.

9.8: Varying the temperature of the coiling process between 575 and 600 ºC did not affect the YS/UTS ratio and the simulated coiling process itself diminished the effect

of cooling rate and decreased the ratio in the case with no prior deformation.

9.9: Prior deformation with a 33% reduction below the T_{nr} in the austenite strongly increased the YS/UTS ratio at all cooling rates from 1 to 34 $^{o}Cs^{-1}$ and overshadowed the effect of microstructures or cooling rate on this ratio.

9.10: Molybdenum additions to Nb-Ti micro alloyed steels did not markedly affect the YS/UTS ratio after a simulated coiling process.

CHAPTER 11 RECOMMENDATIONS FOR FUTURE WORK

1. The influence of the strain rate on the non-recrystallisation temperature in torsion tests at higher strain rates of more than 2.5 s^{-1}, to simulate strip rolling mill strain rates more closely.
2. The use of selected area diffraction pattern analysis and misorientation measurements on acicular ferrite lath structures in thin foil TEM work to determine whether the parallel laths have the same crystal orientation and or habit planes.
3. More thin foil TEM work to confirm the role played by non-metallic inclusions as the preferred nucleation sites for acicular ferrite.
4. Larger variations in the quantity of acicular ferrite in these steels to study the effect of this on the YS/UTS ratio by changing the cooling rate after hot rolling or changing the parameters of the hot rolling schedule.